

Epidemic time series similarity is related to geographic distance and age structure

Tad A Dallas<sup>a,\*</sup>, Grant Foster<sup>a</sup>, Robert L Richards<sup>b</sup> and Bret D Elderd<sup>c</sup>

<sup>a</sup>*Department of Biological Sciences, University of South Carolina, Columbia, SC, 29208*

<sup>b</sup>*Odum School of Ecology, University of Georgia, Athens, GA, 30609*

<sup>c</sup>*Department of Biological Sciences, Louisiana State University, Baton Rouge, LA 70802*

\*Corresponding author: tad.a.dallas@gmail.com

**Running title:** Space, age, and epidemic similarity

**Author contributions:** TAD performed the analysis. All authors contributed to manuscript writing.

**Acknowledgements:** This work has been supported by the U.S. National Science Foundation RAPID grant (NSF-DEB-2031196).

**Data accessibility:** *R* code is available on figshare at  
<https://doi.org/10.6084/m9.figshare.19782406.v1> .

**Keywords:** Epidemic similarity, SARS-CoV2, Age structure, Distance decay

<sup>1</sup> Epidemic time series similarity is related to geographic distance and age struc-  
<sup>2</sup> ture

<sup>3</sup> **Abstract**

<sup>4</sup> More similar locations may have similar infectious disease dynamics. There is clear overlap in  
<sup>5</sup> putative causes for epidemic similarity, such as geographic distance, age structure, and popu-  
<sup>6</sup> lation size. We compare the effects of these potential drivers on epidemic similarity compared  
<sup>7</sup> to a baseline assumption that differences in the basic reproductive number ( $R_0$ ) will translate to  
<sup>8</sup> differences in epidemic trajectories. Using COVID-19 case counts from United States counties,  
<sup>9</sup> we explore the importance of geographic distance, population size differences, and age struc-  
<sup>10</sup> ture dissimilarity on resulting epidemic similarity. We find clear effects of geographic space,  
<sup>11</sup> age structure, population size, and  $R_0$  on epidemic similarity, but notably the effect of age struc-  
<sup>12</sup> ture was stronger than the baseline assumption that differences in  $R_0$  would be most related to  
<sup>13</sup> epidemic similarity. Together, this highlights the role of spatial and demographic processes on  
<sup>14</sup> SARS-CoV2 epidemics in the United States.

15 **Introduction**

16 The most recent pandemic of severe acute respiratory syndrome coronavirus 2 (SARS-CoV2)  
17 has highlighted the pressing need to understand how epidemics emerge and spread, and how epi-  
18 demic models may be used for control and mitigation efforts. Models are used to estimate pa-  
19 rameters of interest, which are then used to calculate composite properties (e.g., basic reproduc-  
20 tion number  $R_0$ ; Brauner *et al.* (2021); Ives & Bozzuto (2021)) and to simulate epidemics under  
21 different mitigation scenarios (e.g., Baker *et al.* (2020); Hinch *et al.* (2021); Sun *et al.* (2020)).  
22 However, these composite pathogen properties are not properties of the pathogen alone, but are  
23 conditional on the host population. Differences in susceptibility and contact patterns among  
24 individuals is critical to pathogen transmission and epidemic trajectories (Yin *et al.*, 2017).  
25 Measures of  $R_0$  – quantifying the approximated number of secondary cases from a single case  
26 in a wholly susceptible host population – based on temporal case counts can hint at these dif-  
27 ferences in individual contact and transmission, but could also suggest differences in pathogen  
28 strain diversity and numerous other factors contributing to epidemic dynamics (Corcoran *et al.*,  
29 2020; Ives & Bozzuto, 2021). Understanding the processes that lead to differing epidemic dy-  
30 namics is a pressing research need, as many of these underlying drivers of estimated  $R_0$  may  
31 potentially change over time or with different intervention strategies (Islam *et al.*, 2021).

32 The SARS-CoV-2 pandemic has created a situation where it may be possible to start to dis-  
33 entangle the role of different factors on resulting epidemic trajectories. For one, county-level  
34 data on infectious case counts provide a means to compare how epidemics progressed at the  
35 county scale, and to compare epidemic trajectories between counties. At a basic level, this al-  
36 lows for the comparison of epidemic trajectories to differences in  $R_0$ , as the larger difference  
37 in  $R_0$  would suggest that the epidemics should be quite dissimilar in their trajectories. For one,  
38  $R_0$  may be estimated from the epidemic time series itself, such that epidemics with similar  $R_0$   
39 would naturally have similar dynamics. However,  $R_0$  is a simple composite measure estimated  
40 from a time series that may belie the influence of mitigation efforts and fluctuating epidemic  
41 dynamics (e.g., COVID-19 case counts appeared in distinct waves, while  $R_0$  estimates do not  
42 use all waves; Ives & Bozzuto (2021)). Apart from similarity in  $R_0$  leading to similar epi-  
43 demics, differences in epidemic trajectories may be driven simply by geographic space between  
44 two epidemics. That is, epidemics should be more similar in nearby counties than in distant

45 counties. This could be driven by several interwoven drivers, which may not be reflected in  
46 differences in estimated  $R_0$ , including spatial autocorrelation in demographics, climatic effects  
47 on transmission, differences in mitigation efforts, or the movement of infectious individuals.

48 But there is an inherent circularity here, in that estimates of  $R_0$  are based on the epidemic  
49 trajectories, such that pairwise differences in  $R_0$  between counties should inherently be related  
50 to differences in epidemic trajectories. This creates an interesting baseline for comparison. That  
51 is, differences in  $R_0$  should hypothetically relate to differences in epidemic trajectory – barring  
52 time-varying  $R_0$  and assuming  $R_0$  can be estimated accurately – simply because  $R_0$  is estimated  
53 from a portion of the epidemic time series. Here, we explore how epidemic trajectories are re-  
54 lated to differences in  $R_0$ , and how other important differences between counties may further  
55 influence epidemic trajectories. Specifically, epidemic trajectories may differ as a function of  
56 geographic distance between counties, and differences in age structure and population size. We  
57 find that there is a clear signal of geographic distance and demographic (population size and  
58 age structure) dissimilarity on resulting epidemic trajectory differences for a set of 3139 US  
59 counties. We compare the strength of these relationships to the potentially circular relation-  
60 ship between epidemic trajectory differences and differences in  $R_0$ , finding that age structure  
61 dissimilarity is more strongly related to epidemic trajectory similarity compared to differences  
62 in  $R_0$ . Together, this suggests an important role for age structure to epidemic emergence and  
63 progression, and highlights the importance of considering the spatial landscape of infectious  
64 disease.

## 65 Methods

66 **COVID-19 epidemic time series data** Time series case data for SARS-CoV-2 were compiled  
67 by the Center for Systems Science and Engineering at Johns Hopkins University Dong, Du &  
68 Gardner (2020) for a set of 3139 United States counties, with recorded case counts every day  
69 for the period between January 22, 2020, and May 9, 2022. These data were then rescaled  
70 to cases per 100,000 residents based on county population estimates from the United States  
71 Census Bureau from 2019 Loftin (2019). County age structure data was also obtained from the  
72 US Census Bureau Loftin (2019), and standardized to sum to one within a given county. Age  
73 structure dissimilarity was estimated as the Euclidean distance between two counties in their

<sup>74</sup> age structure distributions. Estimates of  $R_0$  were obtained from Ives & Bozzuto (2021), which  
<sup>75</sup> were estimated from the epidemic time series directly.

<sup>76</sup> **Dynamic time warping** Dynamic time warping (DTW) is an approach to measure the sim-  
<sup>77</sup> ilarity between two time series based on the notion that there is not an inherent 1:1 matching  
<sup>78</sup> between values in each time series (Berndt & Clifford, 1994), largely applied to problems in  
<sup>79</sup> speech (Amin & Mahmood, 2008) and gait (Boulgouris, Plataniotis & Hatzinakos, 2004) recog-  
<sup>80</sup> nition and comparison. The underlying idea is that the speed of speech or gait could be different,  
<sup>81</sup> while the actual underlying pattern is the same (e.g., the same words can be spoken more quickly  
<sup>82</sup> or with differing amounts of pauses). In our application to infectious disease, there is no reason  
<sup>83</sup> to believe that the pairwise difference in Covid-19 case counts between two counties is *actu-*  
<sup>84</sup> *ally* a measure of how similar the epidemics are, given that the epidemics may have started at  
<sup>85</sup> different times. This fundamental disconnect means that perhaps it is more suitable to attempt  
<sup>86</sup> to match the time series data based on the start of the epidemic or to use an approach which is  
<sup>87</sup> flexible to different epidemic start times, as we do here. By allowing an *elastic* transformation  
<sup>88</sup> of the time series, DTW attempts to minimize the difference between the two trajectories while  
<sup>89</sup> accounting for phase shifts in epidemic dynamics (Figure 1).

$$DTW(x, y) = \min_{\pi \in \mathbf{A}(x, y)} \left( \sum_{(i, j) \in \pi} d(x_i, y_j)^q \right)^{1/q} \quad (1)$$

<sup>90</sup> Here, we want to compare two epidemic time series ( $x$  and  $y$ ), considering an alignment  
<sup>91</sup> path  $\pi$  of all possible paths ( $A_{x,y}$ ), where  $i$  and  $j$  correspond to the position in the time series  
<sup>92</sup> mapping onto the potential alignments, where  $q$  is a normalization constant. The goal is to find  
<sup>93</sup> an alignment which minimizes the overall dissimilarity between the two time series. We use  
<sup>94</sup> the `dtw` R package (Giorgino, 2009), and consider the dissimilarity between the time series to  
<sup>95</sup> be the normalized cumulative dissimilarity between the two time series. There is a possibility  
<sup>96</sup> that the results could be sensitive to the inclusion of many leading or trailing zero counts, where  
<sup>97</sup> epidemics were on a fundamentally different timescale across US counties. While this approach  
<sup>98</sup> should account for this, we explore the effect of truncating the epidemic time series to include 5  
<sup>99</sup> leading and 5 trailing zero values before the calculation of the DTW values. Trimming the time  
<sup>100</sup> series to remove these zero-values did not affect our findings (see Supplementary Material).

101 **What is related to epidemic similarity?** Epidemic similarity was measured by comparing  
102 epidemic time series for every pair of US counties. This creates a pairwise dissimilarity ma-  
103 trix. To project this high-dimensional matrix into lower dimensions for analysis, we used t-  
104 distributed stochastic neighbor embedding (t-SNE), a method that offers a low-dimensional  
105 projection of high-dimensional data (Gisbrecht, Schulz & Hammer, 2015). The result of this  
106 embedding is the production of two t-SNE axes, in which each axis contains one value per US  
107 county, and the distance along each axis relates to epidemic dissimilarity, mapping counties out  
108 along the two axes. This allows us to relate these low-dimensional axes representing epidemic  
109 trajectory similarity to differences between counties in terms of spatial distance, demograph-  
110 ics (e.g., age structure and population size), and estimated epidemic properties ( $R_0$  (Ives &  
111 Bozzuto, 2021)).

112 We used Moran's  $I$  to quantify the effects of geographic distance and age structure dissimi-  
113 larity on resulting epidemic similarity. That is, how similar are epidemics in different counties  
114 as a function of geographic distance between counties or differences in age structure between  
115 counties? Originally designed as a measure of spatial autocorrelation, Moran's  $I$  is essentially  
116 a distance-weighted Pearson's correlation, allowing the relationship between a distance ma-  
117 trix (e.g., pairwise geographic distance between all US counties) and a county-level trait (e.g.,  
118 t-SNE axis values). We related each t-SNE axis – representing the projected epidemic dissim-  
119 ilarity between two US counties – to pairwise matrices of 1) geographic distance between US  
120 counties, 2) age structure dissimilarity, 3) absolute difference in population size, and 4) abso-  
121 lute difference in  $R_0$ . The underlying idea being that counties that are closer to one another,  
122 with similar age structure, and not differing greatly in population size or estimated  $R_0$  (Ives &  
123 Bozzuto, 2021) would also be closer together along t-SNE axes. All distance and dissimilarity  
124 matrices – describing the relative difference in geographic distance, age structure, population  
125 size, and  $R_0$  among US county pairs – were standardized to be bound between 0 and 1, and  
126 inverted, such that the largest distances corresponded to the smallest values. This allows us  
127 to calculate  $z$ -scores based on the null distributions, and to compare these scores across the  
128 different distance/dissimilarity matrices.

129 However, we are fundamentally limited by the almost inherent collinearity between some of  
130 these measures. For instance, geographic distance and age structure dissimilarity were posi-

tively related, based on a Mantel test ( $z = 247, p = 0.001$ ), suggesting that more distant counties also have more dissimilar age structure. We explore this further in the Supplemental Materials, where we use Mantel tests on the pairwise epidemic dissimilarity matrix directly, instead of attempting to project the dissimilarity into two axes using t-SNE. However, regressions of distance matrices are notoriously error-prone (Legendre, Fortin & Borcard, 2015), which is why we present the analyses of the t-SNE axes here. By compressing epidemic similarity into a low-dimensional space, more traditional regression techniques can be used. The results of both analyses are qualitatively similar (see Supplementary Materials for further discussion).

**Reproducibility** *R* code and data to reproduce the analyses is provided at  
<https://doi.org/10.6084/m9.figshare.19782406.v1>

## Results

Pairwise epidemic time series similarity was calculated using dynamic time warping (DTW), which was weakly related to Euclidean distance in epidemic time series, suggesting that this approach was able to capture additional information relative to a more simple distance measure (see Supplemental Materials). The matrix of pairwise DTW values were reduced to two axes using t-SNE (Gisbrecht, Schulz & Hammer, 2015). This low-dimensional representation of site-level epidemic similarity showed clear spatial patterns for the first two t-SNE axes (Figure 2). Interestingly, the spatial patterns adhere to geopolitical (i.e., US state) boundaries in some instances, a phenomenon which may be due to differences between states in case reporting standards and practices (Sen-Crowe *et al.*, 2021), but is worthy of future investigation. The extent to which geographic distance is related to epidemic similarity is difficult to discern, as we observed spatial structure in population age structure differences (Figure S3), as well as clear relationships between  $R_0$  and population size (Figure 3).

**What is related to epidemic dissimilarity?** Despite these difficulties, we find a clear relationship between epidemic similarity and geographic distance, age structure dissimilarity, and differences in population size and  $R_0$  between counties (Table 1). These relationships were estimated using Moran's  $I$ , relating the two axes of epidemic similarity to pairwise matrices describing differences in age structure, geographic distance,  $R_0$ , and population size. Moran's  $I$  is

159 scaled between -1 and 1, where a value of 0 represents a lack of distance-based (or dissimilarity-  
160 based) autocorrelation (either negative or positive). All estimated Moran's  $I$  values in the cur-  
161 rent analysis were positive, suggesting positive spatial autocorrelation for all dissimilarity and  
162 distance matrices examined here. Both t-SNE axes – representing epidemic dissimilarity – were  
163 positively related to 1) geographic distance between US counties, 2) age structure dissimilarity,  
164 3) absolute difference in population size, and 4) absolute difference in  $R_0$  (Table 1). Geographic  
165 distance was more related to both t-SNE axes relative to age structure, population size, and  $R_0$   
166 based on both the raw observed value and the corresponding standardized  $z$ -score (Table 1).  
167 Differences in  $R_0$  between counties showed the next strongest signal in the t-SNE axes, fol-  
168 lowed by age structure dissimilarity (Table 1).

## 169 Discussion

170 Here, we explored how geographic space, demographics, and  $R_0$  influence differences in epi-  
171 demic trajectories for over 3000 United States counties. We expected – and found – that coun-  
172 ties with similar  $R_0$  values tended to have similar epidemics. Independent of this, we found  
173 clear effects of geographic distance between counties and dissimilarities in county age struc-  
174 ture on resulting epidemic trajectories, suggesting that  $R_0$  estimated from case or mortality data  
175 (Ives & Bozzuto, 2021) may not capture the full potential of the epidemic in a given location.  
176 Together, we highlight the importance of considering population demographics, age-specific  
177 contact network structure, and geographic distance when attempting to estimate epidemic tra-  
178 jectories. While we approach the problem as one of pairwise dissimilarity in epidemics, it  
179 may be possible to use similar approaches to recreate an expected epidemic time series for an  
180 unsampled location given information on geography and demography.

181 Spatial structure in both age structure and population sizes precludes the attribution of any  
182 form of causal link between age structure or geographic distance and resulting epidemic trajec-  
183 tories. However, our findings, based on the entire epidemic time, broadly agree with similar  
184 studies which focused on components of the transmission process or summary statistics such  
185 as  $R_0$ . Further, the analyses can be updated as the epidemic progresses, or using different  
186 time windows to explore how time series clustering changes temporally. It is recognized that  
187 both parts of the transmission process – encounter and susceptibility – vary with individual age

(Covid *et al.*, 2020; Jones *et al.*, 2021; Kerr *et al.*, 2021; Magpantay, King & Rohani, 2019), suggesting that for some pathogens including SARS-CoV-2, considering the age structure is quite important to epidemic forecasting (Kerr *et al.*, 2021). Additionally, geographic patterns in  $R_0$  (Ives & Bozzuto, 2021), non-pharmaceutical interventions initiation and compliance (Amuedo-Dorantes, Kaushal & Muchow, 2021; Yang *et al.*, 2021), and vaccine hesitancy (Zuzek, Zipfel & Bansal, 2022) have emerged as potential drivers for spatial variation in epidemic progression (Richards *et al.*, 2022). By comparing epidemic trajectories directly, using a flexible framework which allows epidemics to be sampled at different timescales, we have found that these similarity patterns in summary values, transmission components, and intervention uptake scale up directly to the similarity between entire epidemics.

One major result is the marked state-level clustering of epidemic similarity (Figure 2). Previous clustering of US states was observed early in the pandemic at the state-level (Rojas, Valenzuela & Rojas, 2020), potentially reflecting large scale differences in mitigation protocols (e.g., closing bars and restaurants) or differences in testing regimes across US states. The consistent clustering at US state level when considering counties as the unit of study suggests that state-level variation in reporting, testing, or mitigation may manifest to influence epidemic similarity. Understanding the cause of this clustering may help to inform mitigation efforts, and help to uncover differences in testing or reporting that may be important to understand spatial patterns of infectious disease.

It is interesting that epidemic similarity showed clear signals of geographic distance, age structure, and county-level differences in population size and  $R_0$ , given that counties also varied in other marked ways. For instance, differences in non-pharmaceutical interventions, vaccination rate variation, and other demographic factors which we recognize are important to pathogen spread (Abedi *et al.*, 2021; Ge *et al.*, 2022; Zuzek, Zipfel & Bansal, 2022) did not mask the effect of age structure. One reason for this may be that age structure is serving as a surrogate for other measures of population demography not inherently related to age-structured transmission. That is, differences in vaccination hesitancy (Zuzek, Zipfel & Bansal, 2022) and risk perception (Bruine de Bruin, 2021) may differ across age groups. One way to parse this out would be to examine epidemic trajectory similarity in other geopolitical locations and at different spatial scales, where the relative influence of geographic connectivity, population demographics, and

218 pathogen strain diversity may be quite different. The incorporation of temporal information on  
219 mitigation efforts, strain diversity, and availability of health care infrastructure is a clear next  
220 step to understanding and forecasting epidemic time series. This effort is obviously not aimed at  
221 forecasting directly, but could potentially be used to infer approximate epidemic dynamics for  
222 future epidemics or to explore how deviations from epidemic trajectories between neighboring  
223 counties (or those with similar age structure) may be driven by other critical variables.

224 The COVID-19 pandemic will not be the last pandemic (Medicine, 2022), and understanding  
225 the factors which influence epidemic dynamics are intrinsically important to public health  
226 measures. Perhaps this current pandemic is a special case, as comparisons in  $R_0$  between SARS-  
227 CoV2 and 1918 pandemic influenza revealed little consensus in heavily impacted cities (Foster  
228 *et al.*, 2022). But it seems relevant to use approaches such as the one we do here to understand  
229 how epidemic trajectories differ, both within the same pandemic and potentially for different  
230 pathogens (e.g., how dissimilar are temporal patterns in seasonal flu epidemics in a given lo-  
231 cation?). The comparison of epidemic trajectories – especially along moving windows as the  
232 epidemic progresses – can provide insight into the relative effects of different mitigation and  
233 control efforts. Finally, while many approaches to forecasting epidemics rely on a single time  
234 series, this work alludes to the possibility of incorporating information on nearby or similar  
235 time series, creating the possibility of joint epidemic forecasts.

236 **Conflict of interest:** The authors have no conflicts of interest to declare.

237

238 **Funding source:** This work has been supported by the U.S. National Science Foundation  
239 RAPID grant (NSF-DEB-2031196).

240

241 **Ethical Approval statement:** The present study used publicly available data compiled by the  
242 Center for Systems Science and Engineering at Johns Hopkins University Dong, Du & Gardner  
243 (2020).

## 244 References

245 Abedi, V., Olulana, O., Avula, V., Chaudhary, D., Khan, A., Shahjouei, S., Li, J. & Zand, R.  
246 (2021) Racial, economic, and health inequality and COVID-19 infection in the United States.  
247 *Journal of racial and ethnic health disparities*, **8**, 732–742.

248 Amin, T.B. & Mahmood, I. (2008) Speech recognition using dynamic time warping. *2008 2nd  
249 international conference on advances in space technologies*, pp. 74–79. IEEE.

250 Amuedo-Dorantes, C., Kaushal, N. & Muchow, A.N. (2021) Timing of social distancing poli-  
251 cies and COVID-19 mortality: county-level evidence from the US. *Journal of Population  
252 Economics*, **34**, 1445–1472.

253 Baker, R.E., Park, S.W., Yang, W., Vecchi, G.A., Metcalf, C.J.E. & Grenfell, B.T. (2020) The  
254 impact of COVID-19 nonpharmaceutical interventions on the future dynamics of endemic  
255 infections. *Proceedings of the National Academy of Sciences*, **117**, 30547–30553.

256 Berndt, D.J. & Clifford, J. (1994) Using dynamic time warping to find patterns in time series.  
257 *KDD workshop*, vol. 10, pp. 359–370. Seattle, WA, USA:.

258 Boulgouris, N.V., Plataniotis, K.N. & Hatzinakos, D. (2004) Gait recognition using dynamic  
259 time warping. *IEEE 6th Workshop on Multimedia Signal Processing, 2004.*, pp. 263–266.  
260 IEEE.

261 Brauner, J.M., Mindermann, S., Sharma, M., Johnston, D., Salvatier, J., Gavenčiak, T., Stephen-  
262 son, A.B., Leech, G., Altman, G., Mikulik, V. *et al.* (2021) Inferring the effectiveness of  
263 government interventions against COVID-19. *Science*, **371**.

264 Bruine de Bruin, W. (2021) Age differences in COVID-19 risk perceptions and mental health:  
265 Evidence from a national US survey conducted in March 2020. *The Journals of Gerontology:  
266 Series B*, **76**, e24–e29.

267 Corcoran, D., Urban, M.C., Wegrzyn, J. & Merow, C. (2020) Virus evolution affected early  
268 COVID-19 spread. *medRxiv*.

269 Covid, C., Team, R., COVID, C., Team, R., COVID, C., Team, R., Bialek, S., Boundy, E.,  
270 Bowen, V., Chow, N. *et al.* (2020) Severe outcomes among patients with coronavirus disease

271 2019 (COVID-19) - United States, February 12 - March 16, 2020. *Morbidity and mortality*  
272 *weekly report*, **69**, 343.

273 Dong, E., Du, H. & Gardner, L. (2020) An interactive web-based dashboard to track COVID-19  
274 in real time. *The Lancet infectious diseases*, **20**, 533–534. Publisher: Elsevier.

275 Foster, G., Elderd, B., Richards, R. & Dallas, T. (2022) Estimating  $R_0$  from Early Exponential  
276 Growth: Parallels between 1918 influenza and 2020 SARS-CoV-2 Pandemics. *in review*.

277 Ge, Y., Zhang, W.B., Liu, H., Ruktanonchai, C.W., Hu, M., Wu, X., Song, Y., Ruktanonchai,  
278 N.W., Yan, W., Cleary, E. *et al.* (2022) Impacts of worldwide individual non-pharmaceutical  
279 interventions on COVID-19 transmission across waves and space. *International Journal of*  
280 *Applied Earth Observation and Geoinformation*, **106**, 102649.

281 Giorgino, T. (2009) Computing and Visualizing Dynamic Time Warping Alignments in R: The  
282 dtw Package. *Journal of Statistical Software*, **31**, 1–24.

283 Gisbrecht, A., Schulz, A. & Hammer, B. (2015) Parametric nonlinear dimensionality reduction  
284 using kernel t-SNE. *Neurocomputing*, **147**, 71–82.

285 Hinch, R., Probert, W.J., Nurtay, A., Kendall, M., Wymant, C., Hall, M., Lythgoe, K., Bu-  
286 las Cruz, A., Zhao, L., Stewart, A. *et al.* (2021) OpenABM-Covid19An agent-based model  
287 for non-pharmaceutical interventions against COVID-19 including contact tracing. *PLoS*  
288 *computational biology*, **17**, e1009146.

289 Islam, A., Sayeed, M.A., Rahman, M.K., Zamil, S., Abedin, J., Saha, O. & Hassan, M.M.  
290 (2021) Assessment of basic reproduction number ( $R_0$ ), spatial and temporal epidemiolog-  
291 ical determinants, and genetic characterization of SARS-CoV-2 in Bangladesh. *Infection,*  
292 *Genetics and Evolution*, **92**, 104884.

293 Ives, A.R. & Bozzuto, C. (2021) Estimating and explaining the spread of COVID-19 at the  
294 county level in the USA. *Communications Biology*, **4**, 1–9.

295 Jones, J.M., Stone, M., Sulaeman, H., Fink, R.V., Dave, H., Levy, M.E., Di Germanio, C.,  
296 Green, V., Notari, E., Saa, P. *et al.* (2021) Estimated US infection-and vaccine-induced  
297 SARS-CoV-2 seroprevalence based on blood donations, July 2020-May 2021. *JAMA*, **326**,  
298 1400–1409.

299 Kerr, C.C., Stuart, R.M., Mistry, D., Abeysuriya, R.G., Rosenfeld, K., Hart, G.R., Núñez, R.C.,  
300 Cohen, J.A., Selvaraj, P., Hagedorn, B. *et al.* (2021) Covasim: an agent-based model of  
301 COVID-19 dynamics and interventions. *PLOS Computational Biology*, **17**, e1009149.

302 Legendre, P., Fortin, M.J. & Borcard, D. (2015) Should the Mantel test be used in spatial anal-  
303 ysis? *Methods in Ecology and Evolution*, **6**, 1239–1247.

304 Loftin, L.E. (2019) Overview of the Census Bureau: The Other Nine Years. *The Geography*  
305 *Teacher*, **16**, 103–106.

306 Magpantay, F., King, A. & Rohani, P. (2019) Age-structure and transient dynamics in epidemi-  
307 ological systems. *Journal of the Royal Society Interface*, **16**, 20190151.

308 Medicine, T.L.R. (2022) Future pandemics: failing to prepare means preparing to fail. *The*  
309 *Lancet. Respiratory Medicine*, **10**, 221.

310 Richards, R.L., Foster, G., Elderd, B.D. & Dallas, T.A. (2022) Comparing Waves of COVID-19  
311 in the US: Scale of response changes over time. *medRxiv*.

312 Rojas, F., Valenzuela, O. & Rojas, I. (2020) Estimation of covid-19 dynamics in the different  
313 states of the united states using time-series clustering. *medRxiv*.

314 Sen-Crowe, B., Sutherland, M., McKenney, M. & Elkbuli, A. (2021) The Florida COVID-19  
315 mystery: Lessons to be learned. *The American Journal of Emergency Medicine*, **46**, 661.

316 Sun, J., Chen, X., Zhang, Z., Lai, S., Zhao, B., Liu, H., Wang, S., Huan, W., Zhao, R., Ng,  
317 M.T.A. *et al.* (2020) Forecasting the long-term trend of COVID-19 epidemic using a dynamic  
318 model. *Scientific reports*, **10**, 1–10.

319 Yang, B., Huang, A.T., Garcia-Carreras, B., Hart, W.E., Staid, A., Hitchings, M.D., Lee, E.C.,  
320 Howe, C.J., Grantz, K.H., Wesolowski, A. *et al.* (2021) Effect of specific non-pharmaceutical  
321 intervention policies on SARS-CoV-2 transmission in the counties of the United States. *Na-  
322 ture communications*, **12**, 1–10.

323 Yin, Q., Shi, T., Dong, C. & Yan, Z. (2017) The impact of contact patterns on epidemic dynam-  
324 ics. *PLoS One*, **12**, e0173411.

325 Zuzek, L.G.A., Zipfel, C.M. & Bansal, S. (2022) Spatial clustering in vaccination hesitancy:  
326 the role of social influence and social selection. *medRxiv*.

327 **Tables**

Table 1: Moran's  $I$  analysis exploring how t-SNE axes are related to geographic distance, age structure dissimilarity, difference in population size, and difference in  $R_0$ . Mantel tests use a randomization approach to generate null distributions to compare observed (obs) to null (exp and sd) distributions.  $Z$ -scores estimate the divergence of the test statistic from the null distribution.

covariate	t-SNE axis	obs	exp	sd	p-value	z-score
geography	1	0.02963	-0.00032	0.00014	< <b>0.0001</b>	216.3
	2	0.01930	-0.00032	0.00014	< <b>0.0001</b>	141.7
age structure	1	0.00043	-0.00032	0.00001	< <b>0.0001</b>	60.5
	2	0.00017	-0.00032	0.00001	< <b>0.0001</b>	39.4
population size	1	0.00002	-0.00032	0.00003	< <b>0.0001</b>	11.7
	2	0.00004	-0.00032	0.00003	< <b>0.0001</b>	12.3
$R_0$	1	0.00339	-0.00032	0.00003	< <b>0.0001</b>	110.7
	2	0.00135	-0.00032	0.00003	< <b>0.0001</b>	49.8

328 **Figures**

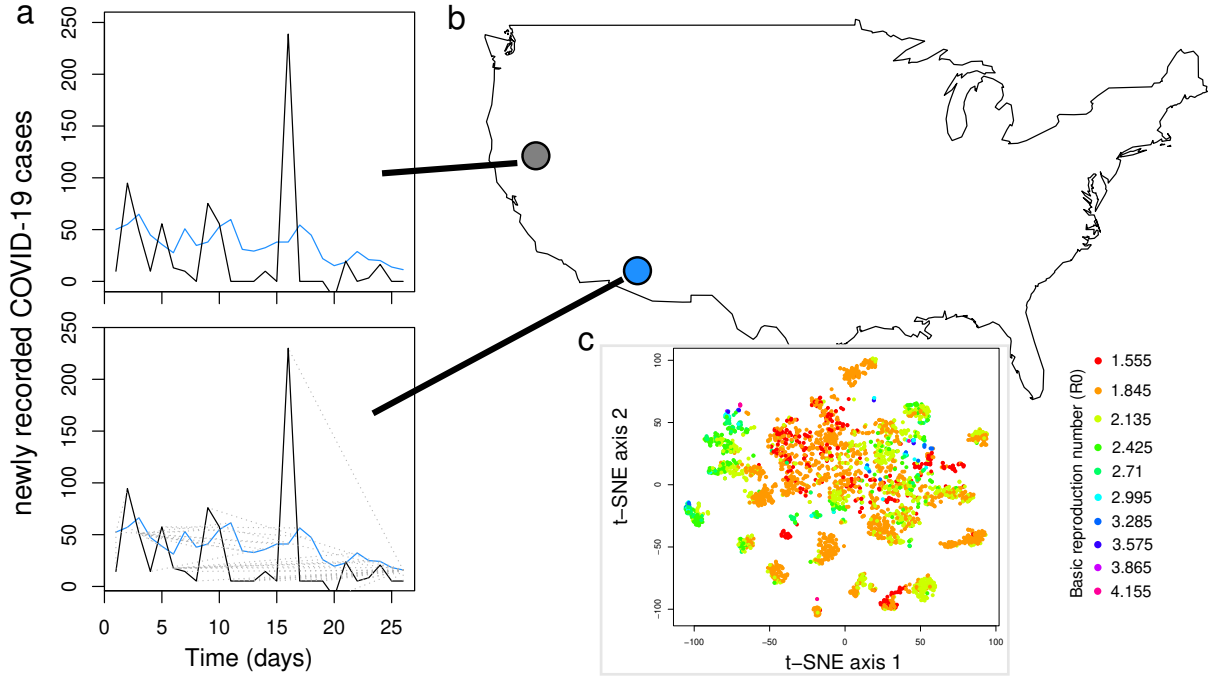


Figure 1: The similarity of epidemic time series was estimated using dynamic time warping, where two time series (in blue and black in panel *a*) are mapped onto one another (indicated by grey lines in panel *a*) to estimate epidemic dissimilarity. These time series are pairwise between every county in the United States (panel *b*). These pairwise values are then compressed to a low-dimensional space by using t-SNE (panel *c*), where point color corresponds to estimated  $R_0$  for the given US county.

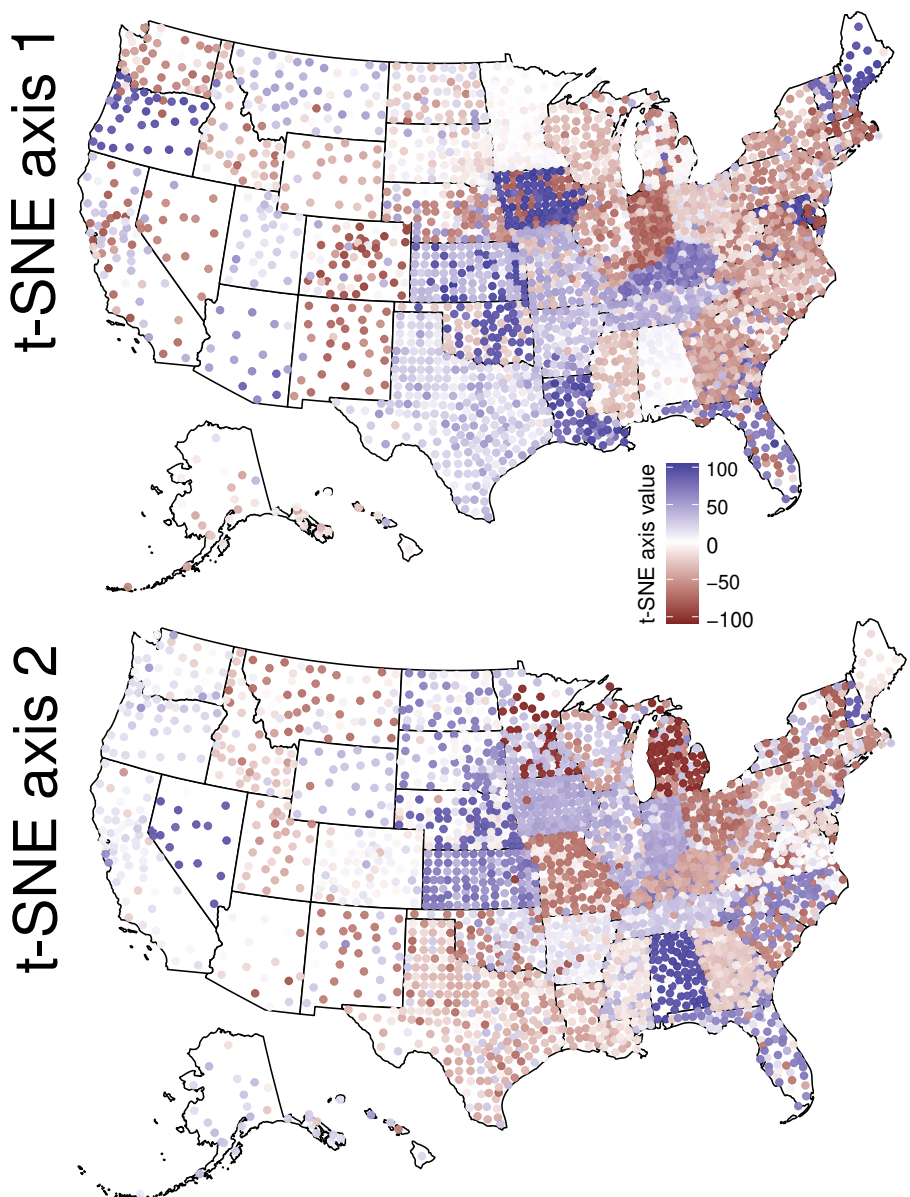


Figure 2: The spatial distribution of epidemic trajectory similarity (t-SNE decomposition of the pairwise dynamic time warping matrix). In this geographic projection of the t-SNE values, there are clearly some states which cluster, suggesting similar mitigation efforts, sampling/reporting biases, and/or epidemic trajectories.

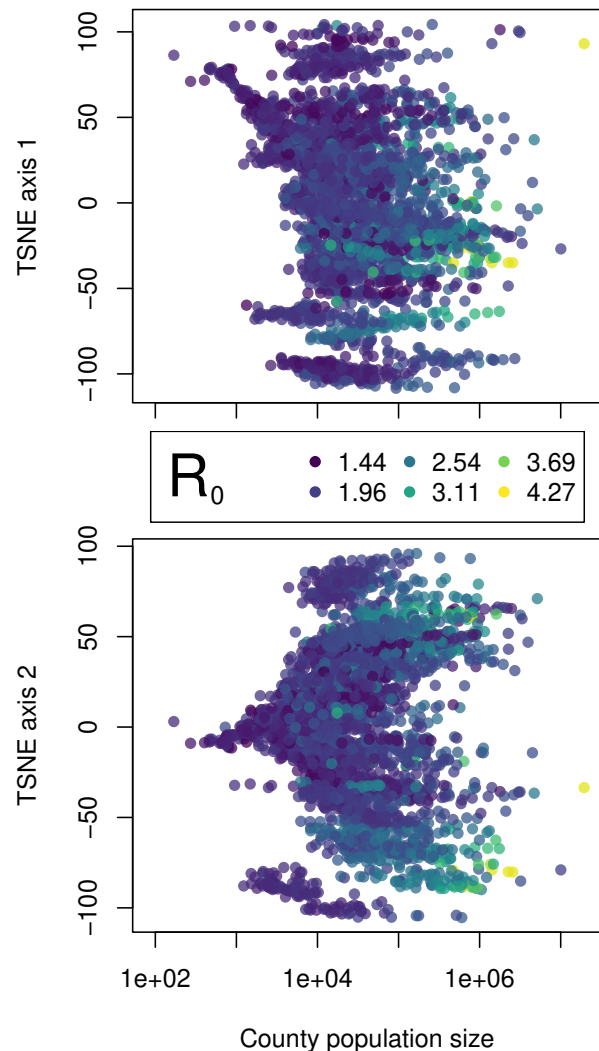


Figure 3: The relationship between t-SNE axes and county population size, with point color corresponding to  $R_0$ , highlighting the distribution of t-SNE values, the messy relationship between epidemic similarity and county population size, and the clear scaling of  $R_0$  with county population size.

329 **Supplementary materials**

330 **Title:** Epidemic time series similarity is related to geographic distance and age structure

331 **Authors:** Tad A Dallas, Grant Foster, Robert Richards, & Bret D Elderd

332 **Does time need to be warped?**

333 We use dynamic time warping as a flexible way to compare time series similarity. Here, we  
334 explore how much of this signal would be observed if we simply calculated the summed differ-  
335 ence in pairwise epidemic trajectories. We found the two approaches are roughly similar, but  
336 that the dynamic time warping does result in different estimates of epidemic similarity (Figure  
337 S1), highlighting the application of such time series approaches to epidemic trajectory data.

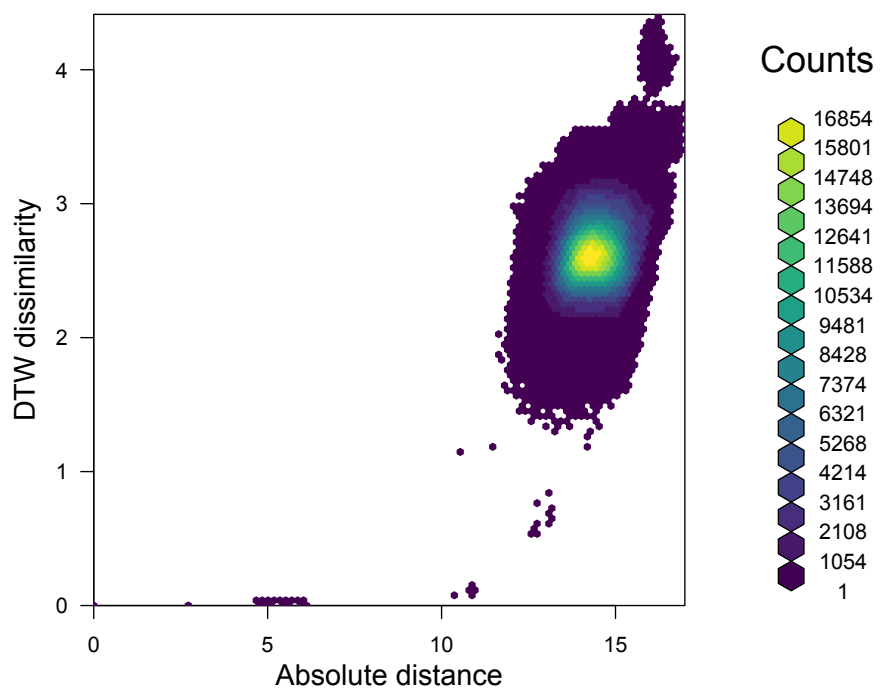


Figure S1: The sum of the absolute difference between the two time series is related to the dynamic time warp dissimilarity in this particular application. There are still clear differences between the two.

338 **Truncating the epidemic time series**

339 In the main text, we considered the full epidemic time series, including case counts in which  
340 case counts were zero-valued. Here, we explore to what extent this influences the dynamic time  
341 warping estimates, and our overall results. This does not influence our overall results (Table  
342 S1), and the two estimates of epidemic dissimilarity produced by truncating the epidemic time  
343 series versus keeping the entire time series are quite positively related (Figure S2).

Table S1: Moran's  $I$  analysis exploring how t-SNE axes are related to geographic distance, age structure dissimilarity, difference in population size, and difference in  $R_0$ . Mantel tests use a randomization approach to generate null distributions to compare observed (obs) to null (exp and sd) distributions.  $Z$ -scores estimate the divergence of the test statistic from the null distribution.

covariate	t-SNE axis	obs	exp	sd	p-value	z-score
geography	1	0.01832	-0.00032	0.00014	< <b>0.0001</b>	134.7
	2	0.02849	-0.00032	0.00014	< <b>0.0001</b>	208.1
age structure	1	0.00041	-0.00032	0.00001	< <b>0.0001</b>	58.9
	2	0.00024	-0.00032	0.00001	< <b>0.0001</b>	45.4
population size	1	0.00001	-0.00032	0.00003	< <b>0.0001</b>	11.2
	2	0.00008	-0.00032	0.00003	< <b>0.0001</b>	13.7
$R_0$	1	0.00231	-0.00032	0.00003	< <b>0.0001</b>	78.6
	2	0.00106	-0.00032	0.00003	< <b>0.0001</b>	41.2

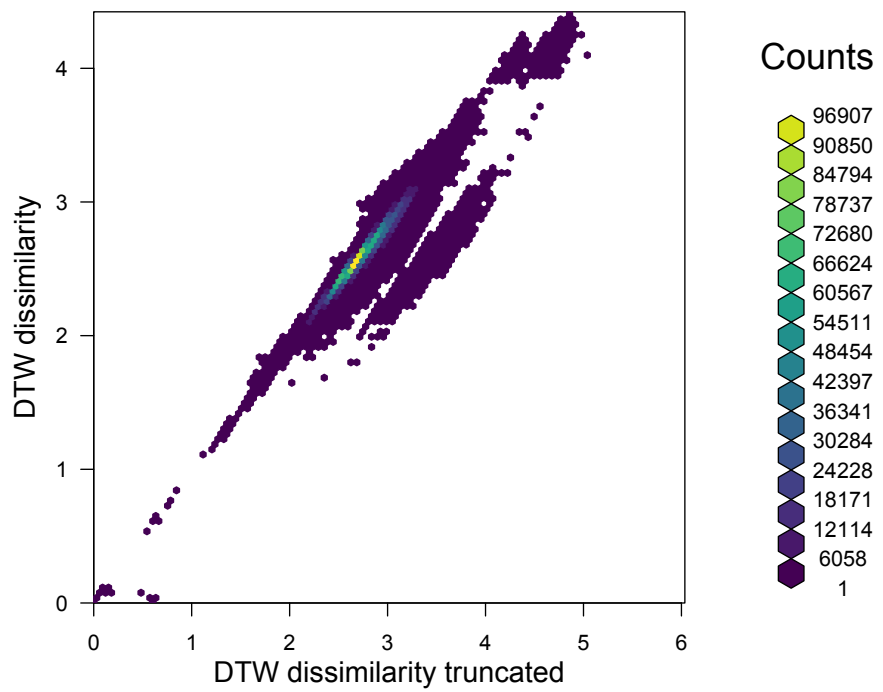


Figure S2: The relationship between dynamic time warping estimates when the time series was truncated to remove the majority of zero values ( $x$ -axis) compared to when the entire epidemic time series was used ( $y$ -axis). Small variations do exist, but this does not affect our overall findings.

344  **$R_0$ , population size, and epidemic similarity**

345 While we can consider epidemics in US counties as being quasi-isolated, with travel restrictions  
346 and differing epidemic timing, it is not possible to control for the inherent link between  $R_0$   
347 (which is estimated from epidemic time series themselves) and population size (Figure S4) and  
348 the resulting epidemic trajectory similarity values obtained from the t-SNE decomposition of  
349 the pairwise dynamic time warping matrix of epidemic similarity.

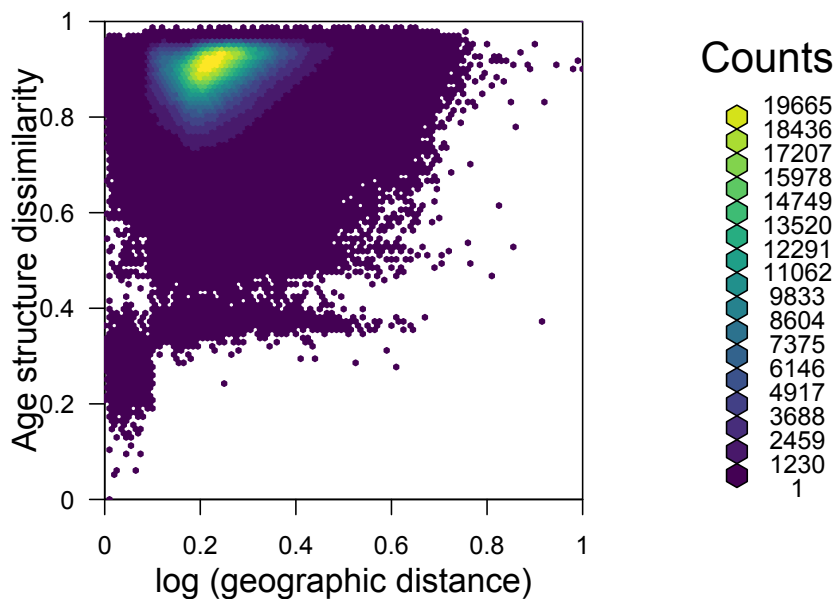


Figure S3: The relationship between geographic distance and age structure dissimilarity.

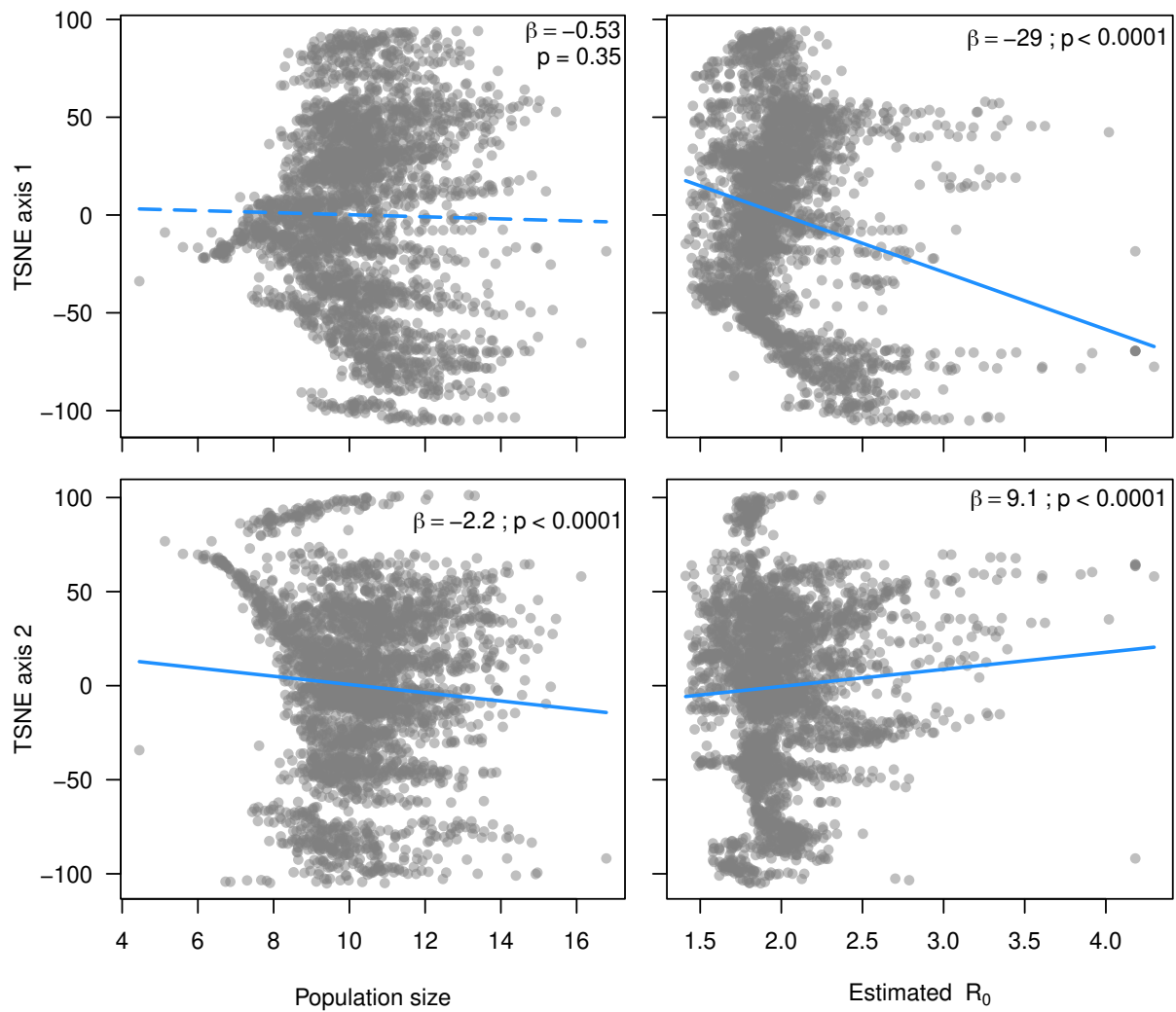


Figure S4: The relationship between epidemic dissimilarity (t-SNE axes as  $y$ -axes) and population size (first column) and estimated  $R_0$  (second column). Blue lines are linear fits (with associated  $\beta$  and  $p$ -values in each panel), where significant lines are solid.

350 **Epidemic similarity as a function of geopolitical boundaries**

351 Epidemic similarity, when compressed to the two t-SNE axes, showed clear US state-level rela-  
352 tionships. There are numerous potential reasons for this, including state-level implementations  
353 of lockdown orders, variation in state-level testing efforts, and variability in reporting. These  
354 are beyond the scope of the current work, but it seems prudent to highlight this variation in  
355 t-SNE space (Figure S5).

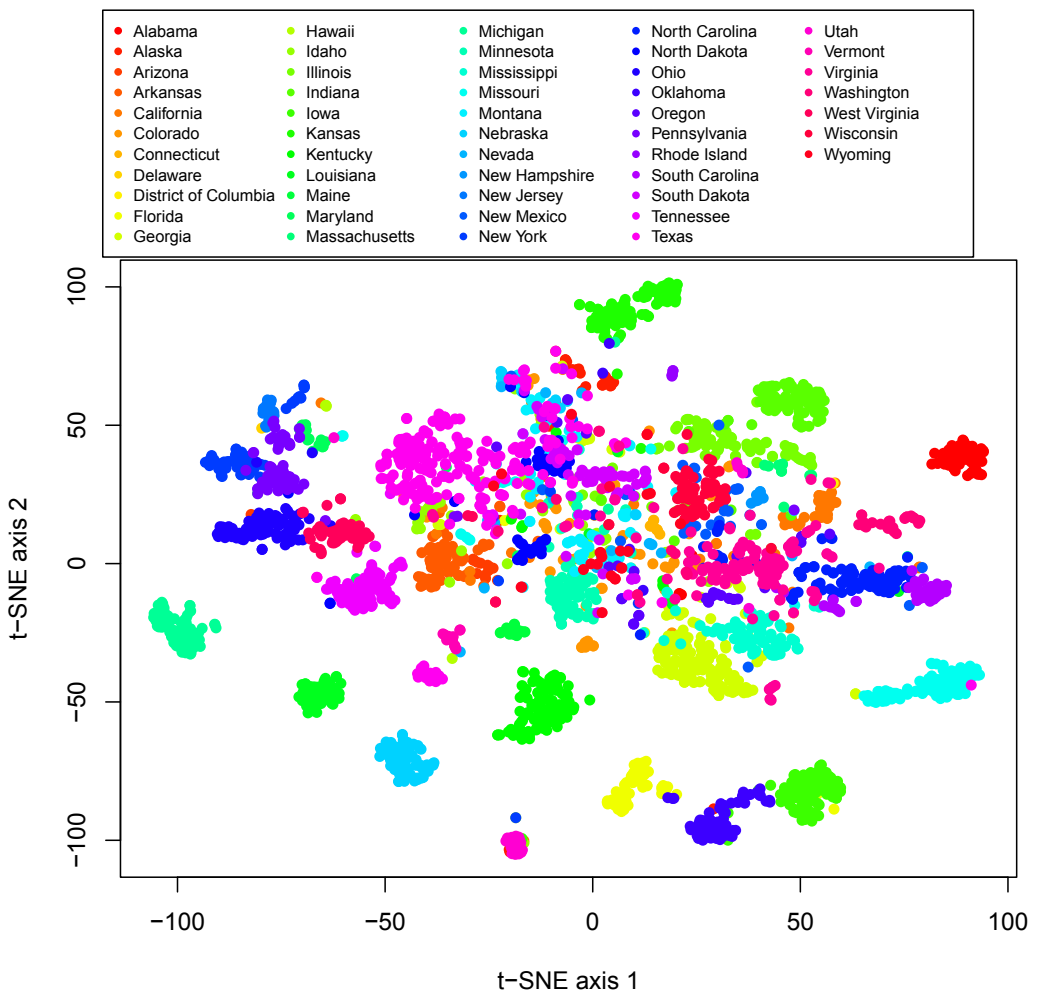


Figure S5: Epidemic similarity in t-SNE space shows clear state-level clustering, suggesting that epidemic similarity was related to some aspect of this geopolitical scale, such as variable mitigation, testing, and reporting efforts.

356 **Mantel Tests**

357 Here, we explore how the pairwise epidemic similarity is related to the distance (or dissim-  
358 ilarity) matrices related to demography and spatial processes. If we claim that  $z$ -score as a  
359 measure of association between epidemic trajectory similarity and geographic distance, age  
360 structure dissimilarity, population size difference, and  $R_0$  difference, then we would conclude  
361 that geographic distance and  $R_0$  difference between US counties are the *most* related to epi-  
362 demic similarity. Each of the distance or dissimilarity matrices were significantly related to the  
363 pairwise epidemic dissimilarity matrix. Taking the estimated  $z$ -score from the Mantel tests as a  
364 measure of association would lead us to conclude that geographic distance was far less impor-  
365 tant than other matrices. Considering the inherent collinearity between many of these variables,  
366 the most salient aspect of this becomes that all of these demographic and spatial factors were  
367 significantly related to epidemic similarity.

Table S2: Mantel tests – permutation tests relating two pair-wise dissimilarities to one another – found that geographic distance, age structure dissimilarity, difference in population size, and difference in  $R_0$  were all related to epidemic trajectory dissimilarity.

covariate	$z$	$p$
geography	3111220	< <b>0.001</b>
age structure	11354792	< <b>0.001</b>
population size	11218853	< <b>0.001</b>
$R_0$	12819318	< <b>0.001</b>